KEK Preprint 2002-66
Belle Preprint 2002-22
NTU-HEP-02-08

arXiv:hep-ex/0207033v2 25 Jul 2002

Measurement of CP-Violating Parameters in $B \to \eta' K$ Decays

Belle Collaboration

K.-F. Chen[aa], K. Hara[af], K. Abe[i], K. Abe[ar], T. Abe[as],
I. Adachi[i], Byoung Sup Ahn[p], H. Aihara[at], M. Akatsu[w],
Y. Asano[az], T. Aso[ay], V. Aulchenko[b], T. Aushev[m],
A. M. Bakich[ao], Y. Ban[ah], A. Bay[s], I. Bedny[b], P. K. Behera[ba],
I. Bizjak[n], A. Bondar[b], A. Bozek[ab], M. Bračko[u,n],
J. Brodzicka[ab], T. E. Browder[h], B. C. K. Casey[h], P. Chang[aa],
Y. Chao[aa], B. G. Cheon[an], R. Chistov[m], S.-K. Choi[g],
Y. Choi[an], Y. K. Choi[an], M. Danilov[m], L. Y. Dong[k],
J. Dragic[v], S. Eidelman[b], V. Eiges[m], Y. Enari[w], F. Fang[h],
C. Fukunaga[av], N. Gabyshev[i], A. Garmash[b,i], T. Gershon[i],
B. Golob[t,n], A. Gordon[v], R. Guo[y], J. Haba[i], K. Hanagaki[ai],
F. Handa[as], T. Hara[af], N. C. Hastings[v], H. Hayashii[x],
M. Hazumi[i], E. M. Heenan[v], I. Higuchi[as], T. Higuchi[at],
L. Hinz[s], Y. Hoshi[ar], W.-S. Hou[aa], Y. B. Hsiung[aa,1],
S.-C. Hsu[aa], H.-C. Huang[aa], T. Igaki[w], Y. Igarashi[i],
T. Iijima[w], K. Inami[w], A. Ishikawa[w], R. Itoh[i], H. Iwasaki[i],
Y. Iwasaki[i], H. K. Jang[am], J. H. Kang[bd], J. S. Kang[p],
N. Katayama[i], H. Kawai[c], Y. Kawakami[w], N. Kawamura[a],
H. Kichimi[i], D. W. Kim[an], Heejong Kim[bd], H. J. Kim[bd],
Hyunwoo Kim[p], T. H. Kim[bd], K. Kinoshita[e], S. Korpar[u,n],
P. Križan[t,n], P. Krokovny[b], R. Kulasiri[e], S. Kumar[ag],
A. Kuzmin[b], Y.-J. Kwon[bd], J. S. Lange[f,aj], G. Leder[ℓ],
S. H. Lee[am], J. Li[aℓ], R.-S. Lu[aa], J. MacNaughton[ℓ],

Preprint submitted to Elsevier Preprint *7 February 2008*

G. Majumder[ap], F. Mandl[ℓ], D. Marlow[ai], T. Matsuishi[w],
S. Matsumoto[d], T. Matsumoto[av], K. Miyabayashi[x],
Y. Miyabayashi[w], H. Miyata[ad], G. R. Moloney[v], T. Mori[d],
A. Murakami[ak], T. Nagamine[as], Y. Nagasaka[j], T. Nakadaira[at],
E. Nakano[ae], M. Nakao[i], J. W. Nam[an], Z. Natkaniec[ab],
S. Nishida[q], O. Nitoh[aw], S. Noguchi[x], S. Ogawa[aq],
T. Ohshima[w], T. Okabe[w], S. Okuno[o], S. L. Olsen[h],
Y. Onuki[ad], W. Ostrowicz[ab], H. Ozaki[i], H. Palka[ab],
C. W. Park[p], H. Park[r], L. S. Peak[ao], J.-P. Perroud[s],
M. Peters[h], L. E. Piilonen[bb], N. Root[b], M. Rozanska[ab],
K. Rybicki[ab], H. Sagawa[i], S. Saitoh[i], Y. Sakai[i], H. Sakamoto[q],
M. Satapathy[ba], A. Satpathy[i,e], O. Schneider[s], S. Schrenk[e],
C. Schwanda[i,ℓ], S. Semenov[m], K. Senyo[w], R. Seuster[h],
M. E. Sevior[v], H. Shibuya[aq], B. Shwartz[b], J. B. Singh[ag],
N. Soni[ag], S. Stanič[az,2], M. Starič[n], A. Sugi[w], A. Sugiyama[w],
K. Sumisawa[i], T. Sumiyoshi[av], S. Suzuki[bc], S. Y. Suzuki[i],
T. Takahashi[ae], F. Takasaki[i], N. Tamura[ad], J. Tanaka[at],
M. Tanaka[i], G. N. Taylor[v], Y. Teramoto[ae], S. Tokuda[w],
M. Tomoto[i], T. Tomura[at], K. Trabelsi[h], W. Trischuk[ai,3],
T. Tsuboyama[i], T. Tsukamoto[i], S. Uehara[i], K. Ueno[aa],
Y. Unno[c], S. Uno[i], Y. Ushiroda[i], G. Varner[h], K. E. Varvell[ao],
C. C. Wang[aa], C. H. Wang[z], J. G. Wang[bb], M.-Z. Wang[aa],
Y. Watanabe[au], E. Won[p], B. D. Yabsley[bb], Y. Yamada[i],
A. Yamaguchi[as], Y. Yamashita[ac], M. Yamauchi[i], H. Yanai[ad],
P. Yeh[aa], M. Yokoyama[at], Y. Yuan[k], Y. Yusa[as], Z. P. Zhang[aℓ],
V. Zhilich[b], and D. Žontar[az]

[a]*Aomori University, Aomori, Japan*
[b]*Budker Institute of Nuclear Physics, Novosibirsk, Russia*
[c]*Chiba University, Chiba, Japan*
[d]*Chuo University, Tokyo, Japan*
[e]*University of Cincinnati, Cincinnati, OH, USA*
[f]*University of Frankfurt, Frankfurt, Germany*
[g]*Gyeongsang National University, Chinju, South Korea*
[h]*University of Hawaii, Honolulu, HI, USA*
[i]*High Energy Accelerator Research Organization (KEK), Tsukuba, Japan*

[j]Hiroshima Institute of Technology, Hiroshima, Japan
[k]Institute of High Energy Physics, Chinese Academy of Sciences, Beijing, PR China
[ℓ]Institute of High Energy Physics, Vienna, Austria
[m]Institute for Theoretical and Experimental Physics, Moscow, Russia
[n]J. Stefan Institute, Ljubljana, Slovenia
[o]Kanagawa University, Yokohama, Japan
[p]Korea University, Seoul, South Korea
[q]Kyoto University, Kyoto, Japan
[r]Kyungpook National University, Taegu, South Korea
[s]Institut de Physique des Hautes Énergies, Université de Lausanne, Lausanne, Switzerland
[t]University of Ljubljana, Ljubljana, Slovenia
[u]University of Maribor, Maribor, Slovenia
[v]University of Melbourne, Victoria, Australia
[w]Nagoya University, Nagoya, Japan
[x]Nara Women's University, Nara, Japan
[y]National Kaohsiung Normal University, Kaohsiung, Taiwan
[z]National Lien-Ho Institute of Technology, Miao Li, Taiwan
[aa]National Taiwan University, Taipei, Taiwan
[ab]H. Niewodniczanski Institute of Nuclear Physics, Krakow, Poland
[ac]Nihon Dental College, Niigata, Japan
[ad]Niigata University, Niigata, Japan
[ae]Osaka City University, Osaka, Japan
[af]Osaka University, Osaka, Japan
[ag]Panjab University, Chandigarh, India
[ah]Peking University, Beijing, PR China
[ai]Princeton University, Princeton, NJ, USA
[aj]RIKEN BNL Research Center, Brookhaven, NY, USA
[ak]Saga University, Saga, Japan
[aℓ]University of Science and Technology of China, Hefei, PR China
[am]Seoul National University, Seoul, South Korea
[an]Sungkyunkwan University, Suwon, South Korea
[ao]University of Sydney, Sydney, NSW, Australia
[ap]Tata Institute of Fundamental Research, Bombay, India
[aq]Toho University, Funabashi, Japan
[ar]Tohoku Gakuin University, Tagajo, Japan

[as] *Tohoku University, Sendai, Japan*
[at] *University of Tokyo, Tokyo, Japan*
[au] *Tokyo Institute of Technology, Tokyo, Japan*
[av] *Tokyo Metropolitan University, Tokyo, Japan*
[aw] *Tokyo University of Agriculture and Technology, Tokyo, Japan*
[ay] *Toyama National College of Maritime Technology, Toyama, Japan*
[az] *University of Tsukuba, Tsukuba, Japan*
[ba] *Utkal University, Bhubaneswer, India*
[bb] *Virginia Polytechnic Institute and State University, Blacksburg, VA, USA*
[bc] *Yokkaichi University, Yokkaichi, Japan*
[bd] *Yonsei University, Seoul, South Korea*

Abstract

We present measurements of CP-violating parameters in $B^0(\overline{B}^0) \to \eta' K^0_S$ and $B^\pm \to \eta' K^\pm$ decays based on a 41.8 fb^{-1} data sample collected at the $\Upsilon(4S)$ resonance with the Belle detector at the KEKB asymmetric-energy e^+e^- collider. We fully reconstruct one neutral B meson as a $B^0(\overline{B}^0) \to \eta' K^0_S$ CP eigenstate and identify the flavor of the accompanying B from its decay products. From the distribution of proper time intervals between pairs of B meson decay points, we obtain the CP-violating asymmetry parameters $\mathcal{S}_{\eta' K^0_S} = 0.28 \pm 0.55(stat)^{+0.07}_{-0.08}(syst)$, and $\mathcal{A}_{\eta' K^0_S} = 0.13 \pm 0.32(stat)^{+0.09}_{-0.06}(syst)$. We also reconstruct charged $B^\pm \to \eta' K^\pm$ decays and determine a direct-CP violating asymmetry value of $\mathcal{A}_{\eta' K^\pm} = (-1.5 \pm 7.0(stat) \pm 0.9(syst))\%$.

Key words: CP Violation, B Decays
PACS: 13.25.Hw, 11.30.Er, 12.15.Hh

In the Kobayashi and Maskawa (KM) model, CP violation is incorporated as an irreducible complex phase in the weak-interaction quark mixing matrix [1]. Measurements of sin2ϕ_1, where $\phi_1 \equiv \pi - \arg(\frac{-V^*_{tb}V_{td}}{-V^*_{cb}V_{cd}})$, from CP violation in $B^0 \to c\bar{c}K^0$ decays by the Belle [2] and BaBar [3] collaborations established CP violation in the neutral B meson system that is consistent with KM expectations. Measurements of sin2ϕ_1 based on other decay modes, especially charmless modes that are mediated by diagrams that contain virtual particle loops, provide important tests of the KM model. In this letter we describe the first measurement of CP-violating asymmetries in the penguin-mediated decay $B^0 \to \eta' K_S^0$, and an improved measurement of the direct CP-violating asymmetry in the decay $B^\pm \to \eta' K^\pm$ [4].

---

[1] on leave from National Fermi Accelerator Laboratory, Batavia, IL, USA
[2] on leave from Nova Gorica Polytechnic, Nova Gorica, Slovenia
[3] on leave from University of Toronto, Toronto, ON, Canada

The KM model predicts CP-violating asymmetries in the time-dependent rates for B^0 and $\overline{B}{}^0$ decay to a common CP eigenstate, f_{CP}. When an $\Upsilon(4S)$ decays into a $B^0\overline{B}{}^0$ meson pair, the two mesons remain in a coherent p-wave state until one of them decays. The decay of one of the B mesons at time $t_{\rm tag}$ to a final state, $f_{\rm tag}$, which distinguishes between B^0 and $\overline{B}{}^0$, projects the accompanying B meson onto the opposite b-flavor which decays to $\eta' K_S^0$ at time t_{CP}. The decay rate has a time dependence given by

$$\mathcal{P}^q_{\eta' K_S^0}(\Delta t) = \frac{e^{-|\Delta t|/\tau_{B^0}}}{4\tau_{B^0}}\{1 + q \cdot A_{CP}(\Delta t)\}, \tag{1}$$

where $A_{CP}(\Delta t)$ is the time-dependent CP asymmetry, τ_{B^0} is the B^0 lifetime, $\Delta t = t_{CP} - t_{\rm tag}$, and the b-flavor $q = +1(-1)$ when the accompanying B meson is a $B^0(\overline{B}{}^0)$.

Within the framework of the Standard Model (SM), the charmless decay $B^0 \to \eta' K_S^0$ proceeds primarily via $b \to s$ penguin diagrams; there is a small contribution from a color-suppressed $b \to u$ tree diagram, but that amplitude is expected to be only a few percent of that for the $b \to s$ penguin [5–7]. Thus, CP violation in this decay mode, to a good approximation, measures ϕ_1, and one can compare the result to the value measured for $B^0 \to (c\overline{c})K_S^0$. Phases from new physics in the penguin loop could show up as a difference between the two measured values [5,8]. Since the branching fraction of $B \to \eta' K$ appears to be anomalously large [9–11], this mode is especially interesting to search for effects of an additional phase besides ϕ_1 due to physics beyond the SM [5].

The time-dependent CP asymmetry can be expressed as

$$\begin{aligned} A_{CP}(\Delta t) &= \frac{\Gamma(\overline{B}{}^0 \to \eta' K_S^0) - \Gamma(B^0 \to \eta' K_S^0)}{\Gamma(\overline{B}{}^0 \to \eta' K_S^0) + \Gamma(B^0 \to \eta' K_S^0)} \\ &= \mathcal{A}_{\eta' K_S^0} \cos(\Delta m \Delta t) + \mathcal{S}_{\eta' K_S^0} \sin(\Delta m \Delta t), \end{aligned} \tag{2}$$

where the CP-violating parameters $\mathcal{A}_{\eta' K_S^0}$ and $\mathcal{S}_{\eta' K_S^0}$ are given by

$$\mathcal{A}_{\eta' K_S^0} = \frac{|\lambda|^2 - 1}{|\lambda|^2 + 1}, \quad \mathcal{S}_{\eta' K_S^0} = \frac{2 Im\lambda}{1 + |\lambda|^2}, \tag{3}$$

in which λ is a complex parameter that depends on both B^0-$\overline{B}{}^0$ mixing and the decay amplitude for $B^0(\overline{B}{}^0) \to \eta' K_S^0$. The SM value for $|\lambda|$ is very nearly equal to the absolute value of the ratio of the $\overline{B}{}^0$ to B^0 decay amplitudes. Therefore $|\lambda| \neq 1$, or equivalently $\mathcal{A}_{\eta' K_S^0} \neq 0$, indicates direct CP violation.

The direct CP asymmetry, $\mathcal{A}_{\eta' K^\pm}$, in charged $B^\pm \to \eta' K^\pm$ decays can also be investigated from the time-integrated decay rates of B^- versus B^+. To a good approximation the CP-violating parameter, $\mathcal{S}_{\eta' K^0_S}$, in the decay $B^0 \to \eta' K^0_S$ is equal to the parameter $\sin 2\phi_1$, which can be directly compared with the value measured from $B^0 \to (c\overline{c})K^0$ decays.

The measurement reported here is based on a 41.8 fb^{-1} data sample, which contains 44.8 million $B\overline{B}$ pairs, collected with the Belle detector at the KEKB asymmetric energy (3.5 GeV on 8 GeV) e^+e^- collider [12] operating at the $\Upsilon(4S)$ resonance. At KEKB, the $\Upsilon(4S)$ is produced with a Lorentz boost of $\beta\gamma = 0.425$ nearly along the electron beam direction (z). Since the B^0 and $\overline{B}^0$ mesons are approximately at rest in the $\Upsilon(4S)$ center-of-mass system, Δt can be determined from the displacement in z between the f_{CP} and $f_{\rm tag}$ decay vertices: $\Delta t \simeq (z_{CP} - z_{\rm tag})/\beta\gamma c \equiv \Delta z/\beta\gamma c$.

The Belle detector is a large solid-angle general purpose magnetic spectrometer that consists of a three-concentric-layer silicon vertex detector (SVD), a 50-layer central drift chamber (CDC), an array of aerogel threshold Čerenkov counters (ACC), time-of-flight scintillation counters (TOF), and an electromagnetic calorimeter comprised of 8736 CsI(Tl) crystals (ECL) located inside a superconducting solenoid coil that provides a 1.5 T magnetic field. An iron flux-return located outside of the coil is instrumented to detect muons and K_L mesons (KLM). The detector is described in detail elsewhere [13].

The $B \to \eta' K$ event selection closely follows the method described in detail in a previously published report that describes the branching ratio measurement [11]; the time-dependent CP analysis is similar to that used for $B^0 \to \pi^+\pi^-$ and presented in Ref. [14].

For the analysis reported here, the event selection is slightly modified for the time-dependent measurement from what described in Ref. [11] in order to retain more signal events and to keep better control of systematic errors. Candidate $K^0_S \to \pi^+\pi^-$ decays are reconstructed from pairs of oppositely charged tracks that are constrained to a common vertex and have an invariant mass that is within ± 16 MeV/c^2 of the nominal K^0_S mass. Two decay channels are used for η' reconstruction: $\eta' \to \eta\pi^+\pi^-$ ($\eta'_{\eta\pi\pi}$) with $\eta \to \gamma\gamma$ ($\eta_{\gamma\gamma}$); and $\eta' \to \rho^0\gamma$ ($\eta'_{\rho\gamma}$) with $\rho^0 \to \pi^+\pi^-$. To increase the event yield, we omit the minimum transverse momentum p_t requirement for charged tracks that was used in Ref. [11]. Instead, we require that all of the tracks have associated SVD hits and radial impact parameters $|dr| < 0.1$ cm projected on the r-ϕ plane. Better tracking requirement improves the vertex determination and gives less bias due to detector asymmetry. Particle identification information from the ACC, TOF and CDC dE/dx measurements are used to form a likelihood ratio in order to distinguish pions from kaons with at least 2.5σ separation for laboratory momenta up to 3.5 GeV/c. Candidate photons from $\eta_{\gamma\gamma}$ ($\eta'_{\rho\gamma}$)

decays are required to be isolated and have $E_\gamma > 50$ (100) MeV from the ECL measurement. The invariant mass of $\eta_{\gamma\gamma}$ candidates is required to be between 500 MeV/c^2 and 570 MeV/c^2. A kinematic fit with an η mass constraint is performed using the fitted vertex of the $\pi^+\pi^-$ tracks from the η' as the decay point. For $\eta'_{\rho\gamma}$ decays, the candidate ρ^0 mesons are reconstructed from pairs of vertex-constrained $\pi^+\pi^-$ tracks with an invariant mass between 550 and 920 MeV/c^2. The η' candidates are required to have a reconstructed mass from 940 to 970 MeV/c^2 for the $\eta'_{\eta\pi\pi}$ mode and 935 to 975 MeV/c^2 for $\eta'_{\rho\gamma}$ mode. Charged $K^\pm$ candidates are selected for the decay $B^\pm \to \eta' K^\pm$ based on the particle identification information described in Ref. [11].

Candidate B mesons are identified by combining η' and K^0_S ($K^\pm$) candidates to form the beam-constrained mass $M_{\rm bc} \equiv \sqrt{(E^{\rm cms}_{\rm beam})^2 - (p^{\rm cms}_B)^2}$, and the energy difference $\Delta E \equiv E^{\rm cms}_B - E^{\rm cms}_{\rm beam}$, where $E^{\rm cms}_{\rm beam}$ is the center of mass (cms) beam energy (nominally 5.29 GeV), and $E^{\rm cms}_B$ and $p^{\rm cms}_B$ are the cms energy and momentum of the B candidate. The $M_{\rm bc}$ signal region is defined as $M_{\rm bc} >$ 5.27 GeV/c^2; the ΔE signal region depends on the mode: it is -0.1 GeV $< \Delta E < 0.08$ GeV for $\eta'_{\eta\pi\pi}$ and $|\Delta E| < 0.06$ GeV for $\eta'_{\rho\gamma}$.

We extract the signal yields with a simultaneous unbinned maximum-likelihood (ML) fit for both ΔE and $M_{\rm bc}$. The signal distribution is a product of a Gaussian function in $M_{\rm bc}$ and a Gaussian plus a bifurcated Gaussian tail function in ΔE. The means and widths, as well as an overall normalization are the fitting parameters. The shapes of the background distributions, described below, are determined from sideband events in the 5.2 GeV/c^2 $< M_{\rm bc} <$ 5.265 GeV/c^2 and $|\Delta E| < 0.25$ GeV region, but with $\Delta E < -0.12$ GeV or $\Delta E > 0.1$ GeV for the $\eta'_{\eta\pi\pi}$ mode and $|\Delta E| > 0.08$ GeV for the $\eta'_{\rho\gamma}$ mode; the difference is due to slight differences in resolution in the data as well as in the Monte Carlo simulation determined from the higher statistics $\eta' K^\pm$ mode.

The dominant backgrounds are from $e^+e^- \to q\overline{q}$ continuum events ($q = u, d, s, c$). In this case, signal and background events can be partially separated by the event topology, which tends to be jet-like for $q\overline{q}$ continuum events and nearly isotropic for $B\overline{B}$ events. We use $|\cos\theta_T|$, the cosine of the angle between the thrust axis of the B candidate and that of the other particles in cms. The requirement $|\cos\theta_T| < 0.9$ rejects 50% of the background while retaining 90% of the signal events. This is sufficient for the $\eta'_{\eta\pi\pi}$ mode, which is relatively clean.

For the $\eta'_{\rho\gamma}$ channel, an additional cut is applied using event shape variables. These variables include $S_\perp$, which is the scalar sum of the transverse momenta of all particles outside a 45° cone around the candidate η' direction divided by the scalar sum of their total momenta, and five modified Fox-Wolfram moments [15], all combined into a single Fisher discriminant. In addition, we use $\cos\theta_B$, the cosine of the angle between the B candidate flight direction

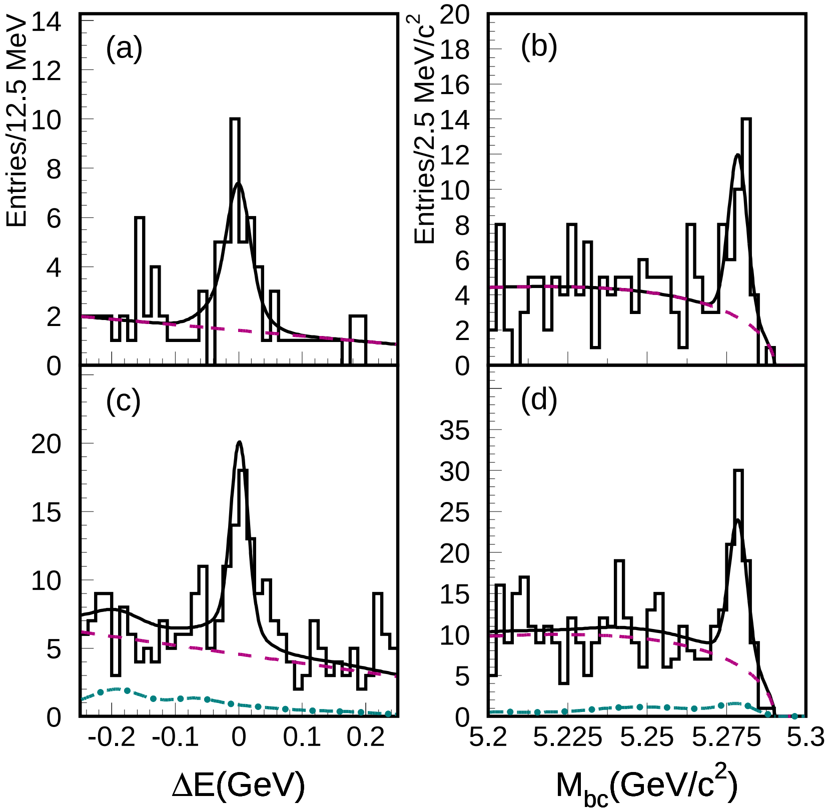

Fig. 1. The ΔE and $M_{\rm bc}$ distributions for the $\eta' K_S^0$ candidates (histogram) and the ML fit results (solid curve); (a) and (b) show the $\eta' \to \eta\pi\pi$ mode, (c) and (d) the $\eta' \to \rho\gamma$ mode. The dashed curves are the results of the fit for $q\overline{q}$ continuum background; the dash-dot curves in (c) and (d) show the expected $B\overline{B}$ background in the $\rho\gamma$ mode from the Monte Carlo simulation.

and the beam axis (z) in the cms, and a ρ helicity variable H, which is the cosine of the angle between the π^+ momentum direction in the ρ rest frame and the ρ momentum direction in the η' rest frame. All of these variables are combined to form a likelihood ratio $LR = L_S/(L_S + L_{q\overline{q}})$, where $L_{S(q\overline{q})}$ is the product of signal ($q\overline{q}$) probability density functions. We determine L_S from Monte Carlo (MC) and $L_{q\overline{q}}$ from sideband data. We require $LR > 0.5$ for the $\eta'_{\rho\gamma}$ mode, which rejects 81% of the background and retains 80% of the signal.

Sideband events are used to determine the shape of the continuum background distributions for the $\eta'_{\eta\pi\pi}$ mode and $\eta'_{\rho\gamma}$ modes separately. The ΔE shape is modelled by a linear background obtained from the $M_{\rm bc}$ sideband. The $M_{\rm bc}$ shape is modelled by the empirical function of Ref. [16]. From the ML fit we determine the total background fraction in the signal region to be 40.4% for the $\eta'_{\eta\pi\pi} K_S^0$ mode and 56.5% for the $\eta'_{\rho\gamma} K_S^0$ mode. The backgrounds are predominantly $q\overline{q}$ continuum events with small contributions from other generic $B\overline{B}$ decays, mainly due to charm daughter particles from B or $\overline{B}$ decay. These backgrounds, which are determined from a sample of MC simulated generic

B meson decays, are negligible for the $\eta'_{\eta\pi\pi}K_S^0$ mode (smaller than 1%), but contribute 14% of the total background for the $\eta'_{\rho\gamma}K_S^0$ mode. The larger background for the $\eta'_{\rho\gamma}K_S^0$ mode is due to wide width of ρ mass and combinatorial background of γ and ρ to form η' candidates.

In the case of multiple candidates from the same event, we select the candidate with the best χ^2 value from the η' mass constrained fit. The signal efficiency is determined from MC events to be 17.2 (16.5)% for $\eta'_{\eta\pi\pi}K_S^0$ ($\eta'_{\rho\gamma}K_S^0$). From the above-described ML fit, we obtain $27.7^{+6.2}_{-5.5}$ signal events in the $\eta'_{\eta\pi\pi}K_S^0$ mode and $45.5^{+8.6}_{-7.9}$ events in the $\eta'_{\rho\gamma}K_S^0$ mode; the results of the fits are shown in Fig. 1.

Leptons, Λ baryons, and charged pions and kaons that are not associated with the reconstructed $B^0 \to \eta' K_S^0$ decay are used to identify the flavor of the accompanying B meson. We apply the same method used for the Belle $\sin 2\phi_1$ measurement [2]. We use two parameters, q and r, to represent the tagging information: q is a discrete variable that corresponds to the sign of the b quark charge and has the value $q = +1$ for a $\overline{b}$ (i.e., B^0) tag, and $q = -1$ for a b ($\overline{B}^0$) tag; r is an event-by-event, MC-determined flavor-tagging dilution factor that ranges from $r = 0$ (no flavor discrimination) to $r = 1$ (unambiguous flavor assignment). The value of r is used to sort data into six intervals of r, according to flavor purity, the corresponding wrong tag fractions, $w_l (l = 1, 6)$, and dilution factors $(1 - 2w_l)$ are determined for each r bin from data as described in Ref. [2].

The vertex positions for the $\eta' K_S^0$ and $f_{\rm tag}$ decays are reconstructed using tracks that have at least one three-dimensional space point determined from associated r-ϕ and z hits in the same SVD layer and one or more additional z hits in the other layers. Each vertex position is required to be consistent with the interaction point profile smeared in the r-ϕ plane by the average transverse B meson decay length. The $f_{\rm tag}$ vertex is determined from all remaining well reconstructed tracks after the $B^0 \to \eta' K_S^0$ candidate tracks are removed. Tracks from other K_S^0 candidates are not used. The MC simulation indicates that the typical combined track-finding and vertex-finding efficiency is 83% for $\eta' K_S^0$ decays and 95% for the $f_{\rm tag}$ decays. The typical vertex resolution (rms) is 147 μm (89 μm) for the $\eta'_{\eta\pi\pi}$ ($\eta'_{\rho\gamma}$) mode on the CP side, and 159 μm for the $z_{\rm tag}$ on the tagging side.

The proper-time interval resolution for the signal, $R_{\rm sig}(\Delta t)$, is obtained by convolving a sum of two Gaussians (a *main* component due to the SVD vertex resolution and charmed meson lifetimes, plus a *tail* component to account for poorly reconstructed tracks) with a function that takes into account the cms motion of the B mesons. The fraction in the main Gaussian is determined to be 0.97 ± 0.02 from a study of control samples of fully reconstructed B^0 mesons [2]. The means ($\mu_{\rm main}$, $\mu_{\rm tail}$) and widths ($\sigma_{\rm main}$, $\sigma_{\rm tail}$) of the Gaussians are calculated event-by-event from the $\eta' K_S^0$ and $f_{\rm tag}$ vertex fit error matrices and the χ^2 values from the fits [17]. The background resolution $R_{q\overline{q}}(\Delta t)$ has the same functional form but the parameters are obtained also event-by-event from the $M_{\rm bc}$ and ΔE sideband events. We obtain the lifetimes for neutral and charged B mesons for the $\eta' K$ channels using the same procedure; the results [18] are consistent with the world average values.

After vertexing, we find 77 candidate events with $q = +1$ (B^0) flavor tags and 74 candidate events with $q = -1$ ($\overline{B}^0$) for $B^0 \to \eta' K_S^0$. Figures 2(a) and 2(b) show the observed Δt distribution for the two samples.

We determine the CP-violating parameters, $\mathcal{A}_{\eta' K_S^0}$ and $\mathcal{S}_{\eta' K_S^0}$, by performing an unbinned ML fit to the observed Δt distributions. For perfect resolution, the probability density function (pdf) for the signal, $\mathcal{P}_{\rm sig}^q$, as a function of $\mathcal{A}_{\eta' K_S^0}$ and $\mathcal{S}_{\eta' K_S^0}$ is given by Eqs. 1 and 2 with q replaced by $q(1-2w_l)$ to take into account the dilution due to mis-tagging. We fix τ_{B^0} and Δm_d at their world average values [19]. The pdf used for the $q\overline{q}$ background distribution is

$$\mathcal{P}_{q\overline{q}}(\Delta t) = \frac{1}{2}\left\{ f_\tau \cdot \frac{e^{-|\Delta t|/\tau_{bg}}}{2\tau_{bg}} + (1-f_\tau)\cdot \delta(\Delta t) \right\}, \tag{4}$$

where f_τ is the background fraction with an effective lifetime τ_{bg} and $\delta(\Delta t)$ is the Dirac delta function. We determine $f_\tau = 0.064 \pm 0.022$ and $\tau_{bg} = 2.24 \pm 0.37$ ps from the sideband data. The pdf used to account for the small generic $B\overline{B}$ background for the $\eta'_{\rho\gamma}$ mode is $\mathcal{P}_{B\overline{B}}(\Delta t) = \delta(\Delta t)/2$. This background is mainly due to mis-reconstructed secondary (charm) decays, such as $D^{(*)0}\rho^\pm$, $D^{(*)\mp}\rho^\pm$, $D^{(*)0}\pi^\pm$ and $D^{(*)}l\nu$, etc. with D mesons decaying into a kaon and multiple pions or a ρ meson.

We define the likelihood value for each event as:

$$\begin{aligned} P_i = \int \Big\{ & f_{\rm sig}^l \mathcal{P}_{\rm sig}^q(\Delta t', w_l) R_{\rm sig}(\Delta t_i - \Delta t') + f_{q\overline{q}}^l \mathcal{P}_{q\overline{q}}(\Delta t') R_{q\overline{q}}(\Delta t_i - \Delta t') \\ & + f_{B\overline{B}}^l \mathcal{P}_{B\overline{B}}(\Delta t') R_{B\overline{B}}(\Delta t_i - \Delta t') \Big\}\, d\Delta t'. \end{aligned} \tag{5}$$

Here f_k^l ($k = {\rm sig}, q\overline{q}$ or $B\overline{B}$ and $l = 1, 6$) are the weighted probability functions determined on an event-by-event basis as a function of ΔE and $M_{\rm bc}$, properly normalized by the average signal and background fractions in the fitting region for each r interval for the signal $\eta' K_S^0$, $q\overline{q}$ and $B\overline{B}$ events, defined as

$$f_k^l(\Delta E, M_{\rm bc}) = \frac{g_k^l F_k^{\Delta E, M_{\rm bc}}}{g_{\rm sig}^l F_{\rm sig}^{\Delta E, M_{\rm bc}} + g_{q\overline{q}}^l F_{q\overline{q}}^{\Delta E, M_{\rm bc}} + g_{B\overline{B}}^l F_{B\overline{B}}^{\Delta E, M_{\rm bc}}}. \tag{6}$$

Here $g_{\rm sig}^l + g_{q\overline{q}}^l + g_{B\overline{B}}^l = 1$ and $F_k^{\Delta E, M_{\rm bc}}$ are the shape functions for the signal ($k = sig$), continuum background ($k = q\overline{q}$) and $B\overline{B}$ background ($k = B\overline{B}$).

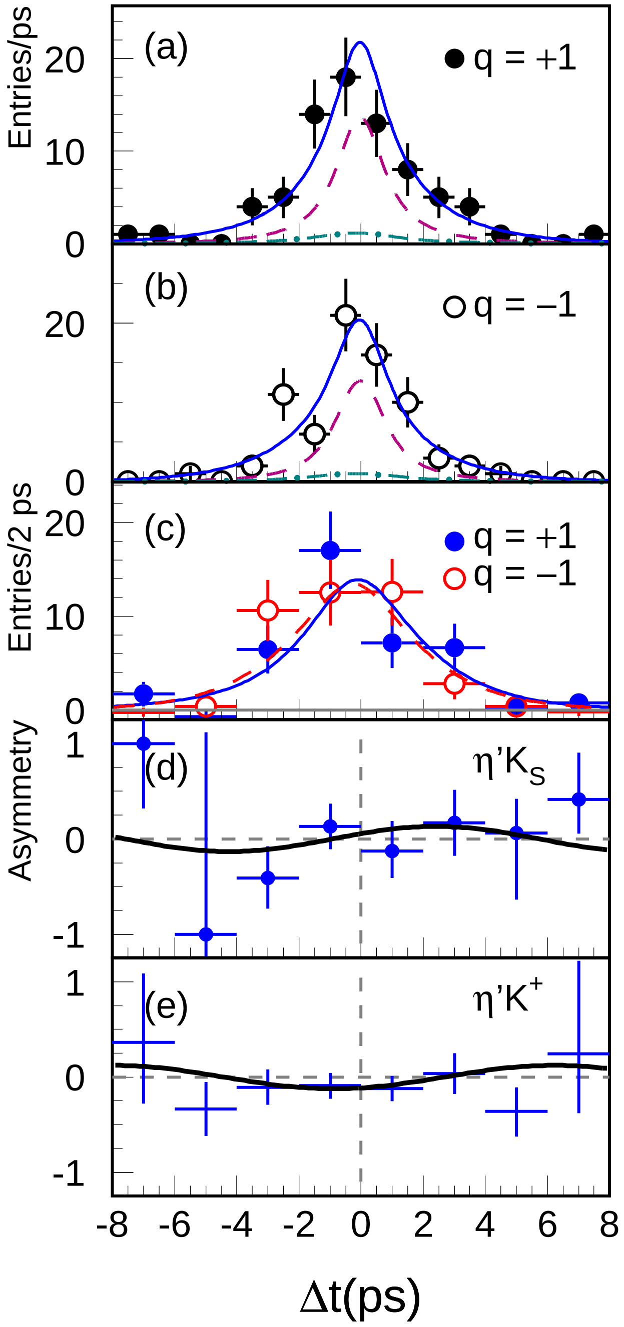

Fig. 2. The Δt distributions for the $B^0 \to \eta' K_S^0$ candidates in the signal region: (a) candidates with $q = +1$, i.e. the tag side is identified as B^0; (b) candidates with $q = -1$; (c) $\eta' K_S^0$ yields after background subtraction; (d) the CP asymmetry for $B^0 \to \eta' K_S^0$ after background subtraction; (e) the same asymmetry calculated for $\eta' K^\pm$ events. The curves in the figures show the results of the unbinned maximum likelihood fit. In (a) and (b), the solid, dashed and dash-dot curves are fit results for the total, $q\overline{q}$ background and $B\overline{B}$ background respectively. In (c) the solid (dashed) curve is for the $q = +1$ ($q = -1$) signal fit. In (d) and (e), the solid curve is the fit result for $\mathcal{A}_{\eta' K_S^0}$ and $\mathcal{S}_{\eta' K_S^0}$ while the dashed curve corresponds to zero asymmetry.

The average event fractions, g_k^l, are measured for $\eta\pi\pi$ and $\rho\gamma$ separately in each r interval.

In the fit, $\mathcal{A}_{\eta' K_S^0}$ and $\mathcal{S}_{\eta' K_S^0}$ are free parameters that are determined by maximizing the likelihood function $\mathcal{L} = \prod_i P_i$, where the product is over all $B^0 \to \eta' K_S^0$ candidates. After maximizing the combined likelihood, the CP asymmetry parameters are determined from a total of 72.9 $\eta' K_S^0$ signal events (37.3 B^0- and 35.6 $\overline{B}^0$-tags) to be:

$$\mathcal{S}_{\eta' K_S^0} = 0.28 \pm 0.55(stat)^{+0.07}_{-0.08}(syst),$$
$$\mathcal{A}_{\eta' K_S^0} = 0.13 \pm 0.32(stat)^{+0.09}_{-0.06}(syst).$$

Figures 2(a) and (b) show the Δt distribution for B^0- and $\overline{B}^0$-tagged events together with the fit curves; the background-subtracted Δt distributions for signal-only are shown in Fig. 2(c). The errors on data points in Fig. 2(c) are statistical only and do not include the error associated with the subtracted background obtained by the fit. The background-subtracted time-dependent CP asymmetry between the B^0- and $\overline{B}^0$-tagged events is shown as a function of Δt in Fig. 2(d), with the result of the fit for $\mathcal{S}_{\eta' K_S^0}$ and $\mathcal{A}_{\eta' K_S^0}$ superimposed.

The systematic errors are summarized in Table 1 for $\mathcal{S}_{\eta' K_S^0}$ and $\mathcal{A}_{\eta' K_S^0}$. The dominant sources for $\mathcal{S}_{\eta' K_S^0}$ are due to uncertainties in the signal and background determination (ΔE and $M_{\rm bc}$ pdf's, event fractions and background shape), resolution functions, wrong tag fractions, vertexing, and the physics parameters (τ_{B^0} and Δm_d). For $\mathcal{A}_{\eta' K_S^0}$, the uncertainties in the signal and background determination and the vertexing are the leading components. We determine the systematic error due to physics parameters by repeating the fit after varying those parameters within their error taken from the world average [19]. The systematic errors for wrong tag fractions, resolution functions, signal and background pdf's are estimated by repeating the fit after varying the parameters by $\pm 1\sigma$ determined from the data or MC. The systematic error due to vertexing is studied by varying the cut on vertex χ^2 or removing it and then repeat the fit.

A number of checks are also performed. We analyze the $\eta' K^\pm$ sample in the same way as $\eta' K_S^0$. The raw asymmetry for the $B^\pm \to \eta' K^\pm$ candidates is shown in Fig. 2(e). A fit to 230 candidate events yields $\mathcal{S} = 0.11 \pm 0.29$ and $\mathcal{A} = -0.27 \pm 0.17$, consistent with no asymmetry, as expected. We also examine the event yields and the Δt distributions for B^0- and $\overline{B}^0$-tagged events in the ΔE and $M_{\rm bc}$ sideband region. We find no significant difference between the two samples in both the $\eta' K^\pm$ and $\eta' K_S^0$ modes. The average raw asymmetry from the sideband data is -0.009 ± 0.014, which is consistent with zero and indicates no bias.

We also analyze the self-tagged $\eta' K^\pm$ event sample to search for a direct

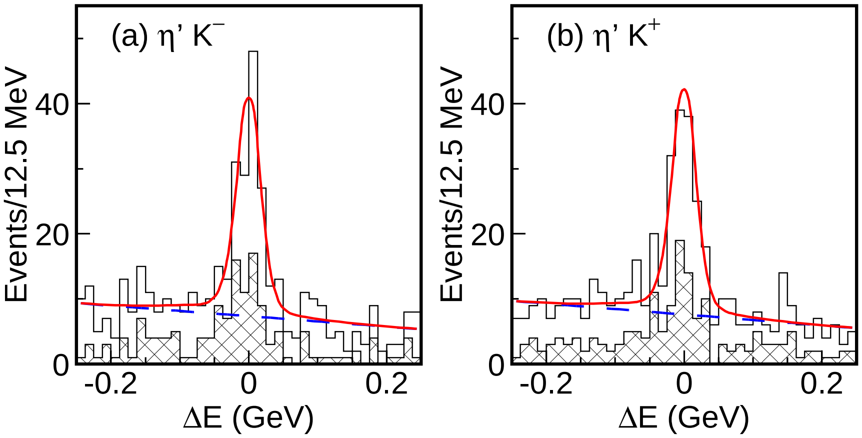

Fig. 3. The ΔE projection plots for the $\eta' K^{\pm}$ candidates: (a) for $\eta' K^-$, (b) for $\eta' K^+$. The cross hatched histograms indicate the $\eta\pi\pi$ channel; the solid histograms are the sum of both η' decay channels ($\eta\pi\pi$ and $\rho\gamma$). The curves are the fitted backgrounds (dashed) and the sum of signal and background (solid).

CP asymmetry. Here we do not use flavor-tag information from the other B meson. The $\eta' K^{\pm}$ sample is divided into $\eta' K^+$ and $\eta' K^-$ samples. Since the CP asymmetry ($\mathcal{A}_{\eta' K^{\pm}} = (N(B^-) - N(B^+))/(N(B^-) + N(B^+))$ for $\eta' K^{\pm}$ is time independent, we use the same event selection and analysis procedure as described in Ref. [11]. A simultaneous ML fit to $M_{\rm bc}$ and ΔE is performed for each sub-sample. The fitted numbers of signal events in the $\eta'_{\eta\pi\pi}$ ($\eta'_{\rho\gamma}$) mode are $66.0^{+10.0}_{-9.2}$ ($73.7^{+14.3}_{-13.5}$) for B^- decays and $66.6^{+10.1}_{-9.3}$ ($77.5^{+10.8}_{-10.0}$) for B^+ decays, respectively. The number of produced B^- and B^+ events are obtained by maximizing the product of the likelihoods for each submode, as shown in Fig. 3. From the fit we obtain $\mathcal{A}_{\eta' K^{\pm}} = (-0.4 \pm 11.0)\%$ for the $\eta'_{\eta\pi\pi}$ mode and $(-2.5 \pm 10.0)\%$ for $\eta'_{\rho\gamma}$; here the errors are statistical only. Since the systematic errors on η' reconstruction and the number of $B\overline{B}$ events cancel in the ratio, the systematic uncertainty in $\mathcal{A}_{\eta' K^{\pm}}$ comes mainly from the reconstruction efficiency of charged kaons and the ML fit. The asymmetry in the $K^{\pm}$ efficiency is studied using inclusive charged kaons in the same kinematic range as the signal. The uncertainty due to fitting is measured by varying the parameters of the fit functions. We find the systematic errors in $\mathcal{A}_{\eta' K^{\pm}}$ are 0.85% from $K^{\pm}$ reconstruction and 0.47% from the ML fit. The combined $\mathcal{A}_{\eta' K^{\pm}}$ for the $B^{\pm} \to \eta' K^{\pm}$ decay is determined to be

$$\mathcal{A}_{\eta' K^{\pm}} = (-1.5 \pm 7.0(stat) \pm 0.9(syst))\%,$$

which is consistent with zero. Combining the errors in quadrature and assuming a Gaussian distribution, we find the 90% confidence level interval is $-0.13 < \mathcal{A}_{\eta' K^{\pm}} < 0.10$, which is a factor of two more restrictive than our previous measurement [11].

In summary, we have measured the CP asymmetry parameters in $B^0(\overline{B}^0) \to$

$\eta' K^0_S$ and $B^\pm \to \eta' K^\pm$ decays based on a 41.8 fb^{-1} data sample collected with the Belle detector. The result for decay-time-integrated direct CP asymmetry, $\mathcal{A}_{\eta' K^\pm} = (-1.5 \pm 7.0(stat) \pm 0.9(syst))\%$, is small and consistent with zero. Our results for the time-dependent asymmetry parameters $\mathcal{S}_{\eta' K^0_S} = 0.28 \pm 0.55(stat)^{+0.07}_{-0.08}(syst)$ and $\mathcal{A}_{\eta' K^0_S} = 0.13 \pm 0.32(stat)^{+0.09}_{-0.06}(syst)$ are the first measurements of CP asymmetry parameters related to ϕ_1 with a charmless B^0 decay mode. In the SM, to a good approximation the value of $\mathcal{S}_{\eta' K^0_S}$ should be equal to $\sin 2\phi_1$ measured in $B^0 \to c\bar{c}K^0$ decays, where the current world average is 0.78 ± 0.08 [20]. With a much larger data sample, we will significantly reduce the uncertainty in $\mathcal{S}_{\eta' K^0_S}$ and impose tight constraints on phases from new physics beyond the Standard Model.

We wish to thank the KEKB accelerator group for the excellent operation of the KEKB accelerator. We acknowledge support from the Ministry of Education, Culture, Sports, Science, and Technology of Japan and the Japan Society for the Promotion of Science; the Australian Research Council and the Australian Department of Industry, Science and Resources; the National Science Foundation of China under contract No. 10175071; the Department of Science and Technology of India; the BK21 program of the Ministry of Education of Korea and the CHEP SRC program of the Korea Science and Engineering Foundation; the Polish State Committee for Scientific Research under contract No. 2P03B 17017; the Ministry of Science and Technology of the Russian Federation; the Ministry of Education, Science and Sport of the Republic of Slovenia; the National Science Council and the Ministry of Education of Taiwan; and the U.S. Department of Energy.

References

[1] M. Kobayashi and T. Maskawa, Prog. Theor. Phys. 49 (1973) 652.

[2] Belle Collaboration, K. Abe *et al.*, Phys. Rev. Lett. 87 (2001) 091802; A. Abashian *et al.*, Phys. Rev. Lett. 86 (2001) 2509; and K. Abe *et al.*, hep-ex/0202027, to be published in Phys. Rev. D.

[3] BaBar Collaboration, B. Aubert *et al.*, Phys. Rev. Lett. 87 (2001) 091801; B. Aubert *et al.*, Phys. Rev. Lett. 86 (2001) 2515; and B. Aubert *et al.*, hep-ex/0201020, to be published in Phys. Rev. D.

[4] Charge conjugate modes are implicitly included throughout the paper unless explicitly stated.

[5] D. London and A. Soni, Phys. Lett. B 407 (1997) 61.

[6] A. Ali, G. Kramer and C.-D. Lu, Phys. Rev. D 59 (1999) 014005.

[7] E. Kou and A. I. Sanda, Phys. Lett. B 525 (2002) 240.

[8] T. Moroi, Phys. Lett. B 493 (2000) 366.

[9] CLEO Collaboration, S. J. Richichi *et al.*, Phys. Rev. Lett. 85 (2000) 520.

[10] BaBar Collaboration, B. Aubert *et al.*, Phys. Rev. Lett. 87 (2001) 221802.

[11] Belle Collaboration, K. Abe *et al.*, Phys. Lett. B 517 (2001) 309.

[12] E. Kikutani ed., KEK Preprint 2001-157 (2001), to appear in Nucl. Inst. and Meth. A.

[13] Belle Collaboration, A. Abashian *et al.*, Nucl. Inst. and Meth. A 479 (2002) 117.

[14] Belle Collaboration, K. Abe *et al.*, KEK Preprint 2002-6 and hep-ex/0204002, submitted to Phys. Rev. Lett.

[15] The Fox-Wolfram moments were introduced in G. C. Fox, S. Wolfram, Phys. Rev. Lett. 41 (1978) 1581. The Fisher discriminant used by Belle in this analysis is described in [11].

[16] The functional form is $x\sqrt{1-x^2}e^{\alpha(1-x^2)}$, where $x = M_{\rm bc}/E^{\rm cms}_{\rm beam}$. H. Albrecht *et al.* (ARGUS Collaboration), Phys. Lett. B 241 (1990) 278; 254 (1991) 288.

[17] Typical values are $\mu_{\rm main} = -0.24$ ps, $\mu_{\rm tail} = -0.37$ ps and $\sigma_{\rm main} = 1.06$ ps, $\sigma_{\rm tail} = 3.22$ ps.

[18] We obtain $\tau_{B^\pm} = 1.54 \pm 0.14(stat)$ ps for the $\eta' K^\pm$ mode (the world average [19] is 1.653 ± 0.028 ps) and $\tau_{B^0} = 1.58 \pm 0.30(stat)$ ps for the $\eta' K^0_S$ mode (the world average is 1.548 ± 0.032 ps).

[19] Particle Data Group, D. E. Groom *et al.*, Eur. Phys. J. C 15 (2000) 1.

[20] This average includes recent updated results from Belle: T. Higuchi, hep-ex/0205020; and BaBar: B. Aubert *et al.*, hep-ex/0203007.

Table 1

Summary of systematic errors.

Source	$\delta(\mathcal{S}_{\eta' K_S^0})$	$\delta(\mathcal{A}_{\eta' K_S^0})$
τ_{B^0} and Δm_d	$^{+0.029}_{-0.034}$	$^{+0.006}_{-0.003}$
Wrong tag fractions	$^{-0.028}_{-0.025}$	$^{+0.013}_{-0.012}$
Resolution functions	$^{+0.037}_{-0.033}$	$^{+0.011}_{-0.008}$
Vertexing	$^{+0.018}_{-0.033}$	$^{+0.062}_{-0.031}$
Event fractions	$^{+0.029}_{-0.024}$	$^{+0.012}_{-0.010}$
Background shapes	$^{+0.013}_{-0.017}$	$^{+0.004}_{-0.003}$
ΔE and $M_{\rm bc}$ pdf's	$^{+0.032}_{-0.028}$	$^{+0.063}_{-0.054}$
Total	$^{+0.07}_{-0.08}$	$^{+0.09}_{-0.06}$